

Input-Output History Feedback Controller for Encrypted Control with Leveled Fully Homomorphic Encryption

K. Teranishi ^{a,b}, T. Sadamoto ^a, K. Kogiso ^a

^a*Department of Mechanical and Intelligent Systems Engineering, The University of Electro-Communications, 1-5-1 Chofugaoka, Chofu, Tokyo 182-8585, Japan*

^b*Research Fellow of Japan Society for the Promotion of Science*

Abstract

Protecting the parameters, states, and input/output signals of a dynamic controller is essential for securely outsourcing its computation to an untrusted third party. Although a fully homomorphic encryption scheme allows the evaluation of controller operations with encrypted data, an encrypted dynamic controller with the encryption scheme destabilizes a closed-loop system or degrades the control performance due to overflow. This paper presents a novel controller representation based on input-output history data to implement an encrypted dynamic controller that operates without destabilization and performance degradation. An algorithm for efficient encrypted control computation is also proposed using single instruction/multiple data operations based on a batching technique. Furthermore, this study analyzes the stability and performance degradation of a closed-loop system caused by the effects of controller encryption. A numerical simulation demonstrates the feasibility of the proposed encrypted control scheme, which inherits the control performance of the original controller at a sufficient level.

Key words: Network security, networked control systems, digital implementation, data-based control, time-invariant.

1 Introduction

The development of cloud computing technologies has promoted outsourcing computation of resource-limited devices, as well as data storage. Control as a service (CaaS) is a concept of cloud-based control that outsources decision-making and monitoring of controlled devices to remote servers, and it is introduced to several control systems, such as automation [13], robotics [29], and automobiles [9]. CaaS has the advantages of scalability and efficiency in terms of energy and costs. However, such control induces security concerns that confidential information of control recipes and privacy of controlled devices can be exposed to an untrusted third party.

Homomorphic encryption [1] is the major approach for establishing secure outsourcing computation while maintaining the confidentiality of a computation process by allowing the direct evaluation of mathematical arithmetic on encrypted data without decryp-

tion. An encrypted control framework [5] was introduced in the literature on control engineering to apply homomorphic encryption for several control operations [2, 6, 7, 11, 12, 17, 20, 26, 27]. Encrypted control can reduce the vulnerabilities induced by CaaS because the controller parameters and control signals over networks are encrypted while a controller server does not have a decryption key.

1.1 Problem of encrypting dynamic controller

Most of the studies on encrypted control considered the encryption of static or linear controllers by using additive or multiplicative homomorphic encryption [5, 11, 20], where the encrypted controller states were decrypted on the plant side at every sampling period. However, encrypting dynamic controllers without temporary decryption remains challenging because it causes an overflow of the states to be encrypted. The majority of homomorphic encryption schemes operate using integers rather than real numbers, and thus controller states and other signals should be quantized before encryption. To deal with this quantization, some studies used binary representation of fractional numbers [6, 11] or rounding of real numbers to the nearest element in a plaintext space af-

* This paper was not presented at any IFAC meeting. Corresponding author K. Teranishi.

Email addresses: teranishi@uec.ac.jp (K. Teranishi), sadamoto@uec.ac.jp (T. Sadamoto), kogiso@uec.ac.jp (K. Kogiso).

ter scaling [20, 28]. The former increases the number of bits for the representation by recursively updating the controller states with homomorphic operations [24]. It is also inevitable for the later that a value of the scaling parameter is accumulated for every homomorphic operation. These effects induce overflow when a dynamic controller is naively encrypted because a plaintext space is a finite set. Once overflow occurs, the decrypted state has to be significantly different from the correct value, thereby easily inducing instability of the encrypted control systems.

To overcome this problem, the authors of [24] proposed a controller that resets its states at a constant period to clear an increase of the number of bits. However, such reset operation obviously degrades the control performance. Another approach in [16] employed fully homomorphic encryption for encrypting dynamic controllers. Fully homomorphic encryption enables to evaluate any arithmetic operations over a ciphertext space. Thus, encrypted dynamic controllers can be implemented using fully homomorphic encryption because the accumulation of scaling parameters can be removed by division over a ciphertext space. However, fully homomorphic encryption requires bootstrapping, which is a technique used to manage noise in a ciphertext. Bootstrapping requires a large amount of computation time and resources to be performed, and therefore the realization of such encrypted control in real time is difficult in practice. Note that, in fully homomorphic encryption, a small noise is injected into a ciphertext to guarantee security. This noise grows every homomorphic operation, and the decryption result includes a large error when the noise reaches a certain size. Hence, bootstrapping is essential for correct computation while ensuring security.

Recent studies [18, 19] reformulated a dynamic controller by pole placement and transformation to a modal canonical form so that its system matrix becomes an integer matrix. This transformation makes quantization of the system matrix unnecessary, and thus the scaling parameter for the controller states does not accumulate. Moreover, these studies considered an error caused by the overflow of injected noises in fully homomorphic encryption as an external disturbance for a closed-loop system. When the dynamic controller is stable under the disturbance, bootstrapping for fully homomorphic encryption was found to be unnecessary for the infinite-time-horizon operation of the controller. Therefore, this approach is promising for implementing an encrypted dynamic controller without decrypting the controller states. However, the external disturbance caused by the injected noise degrades the control performance. Note that, although the criteria for choosing parameters for quantization and encryption were determined so that the perturbation of a control input became smaller than a certain level [19], the stability and control performance of the closed-loop system were not guaranteed.

1.2 Contribution

The contribution of this study to the implementation of an encrypted dynamic controller that does not overflow without considering ciphertext noise as a disturbance is as follows. First, the study presents a novel controller representation using input/output history data of a controller to eliminate the controller states. The intrinsic difficulty of encrypting a dynamic controller stems from the hardness of the recursive update of the encrypted controller states without decryption. To overcome this difficulty, the controller representation adopts the form of a product between a controller parameter matrix and a vector that consists of history data.

Second, a batching technique is used to reduce the computational complexity of leveled fully homomorphic encryption based on ring learning with errors [23] for encrypting the controller. Leveled fully homomorphic encryption does not require bootstrapping, and thus it is more suitable for real-time systems than fully homomorphic encryption. Owing to the batching technique, the number of encryption and decryption in the proposed encrypted control algorithm becomes almost scale-independent, that is, it does not depend on the dimensions of the input and output signals. However, the batching technique makes updating history data of the controller representation impossible. To solve this problem, we propose an encryption-aware modification of the controller representation.

Third, analysis of the effects of quantization errors due to encryption is performed. Such quantization effects may cause destabilization of the encrypted control systems and degradation of the control performance [5]. Herein, we clarify a condition so that an encrypted control system inherits the stability of the original control system. Furthermore, the degree of performance degradation in the worst case is guaranteed as an upper bound of the output trajectory error between the encrypted and unencrypted control systems.

1.3 Outline

The remainder of this paper is organized as follows. Section 2 introduces the notations and leveled fully homomorphic encryption used in this paper. Section 3 presents a novel controller representation using the input-output history data for encrypted control. Section 4 proposes an encrypted control scheme that operates for an infinite time horizon without overflow using the novel controller representation. Section 5 analyzes the effects of quantization by encrypting the controller for stability and performance degradation of a closed-loop system. Section 6 shows the result of a numerical simulation. Section 7 describes the conclusions of this study and future work.

2 Preliminaries

2.1 Notation

The sets of real numbers and integers are denoted by \mathbb{R} and \mathbb{Z} , respectively. For $n > 1$, \mathbb{Z}_n denotes the set of integers $\{z \in \mathbb{Z} \mid -n/2 < z \leq n/2\}$. A polynomial ring R is defined as $R := \mathbb{Z}[X]/(X^N + 1)$, where N is a power of 2. The set of polynomials in R with coefficients in \mathbb{Z}_n is denoted by R_n . For $x \in \mathbb{R}$ and $z \in \mathbb{Z}$, the symbols $\lfloor \cdot \rfloor$ and $[\cdot]_n$ are defined by $\lfloor x \rfloor = \lfloor x + 1/2 \rfloor$ and $[z]_n = z \bmod n$, where $\lfloor \cdot \rfloor$ is the floor function. Similarly, $[\mathbf{a}]_n$ denotes the polynomial in R_n given by applying $[\cdot]_n$ to all coefficients of $\mathbf{a} \in R$. The sets of n -dimensional real-valued vectors and m -by- n real-valued matrices are denoted by \mathbb{R}^n and $\mathbb{R}^{m \times n}$, respectively. The n -dimensional zero row vector and m -by- n zero matrix are denoted by $\mathbf{0}_n$ and $O_{m \times n}$, respectively. The i th element of vector $v \in \mathbb{R}^n$ is denoted by v_i . The (i, j) entry of matrix $M \in \mathbb{R}^{m \times n}$ is denoted by M_{ij} . The ℓ_2 norm of v and the induced 2-norm of M are denoted by $\|v\|$ and $\|M\|$, respectively. The vectorization of M is defined by $\text{vec}(M) := [M_1^\top \cdots M_n^\top]^\top$, where M_i is the i th column vector of M , and M_i^\top is the transpose matrix of M_i . The spectral radius of M is denoted by $\rho(M)$.

2.2 Brakerski/Fan-Vercauteren encryption scheme

This section provides an overview of the Brakerski/Fan-Vercauteren (BFV) leveled fully homomorphic encryption scheme [10] used in this study. The plaintext space of the BFV scheme is a polynomial ring, which is beneficial for the effective encryption/decryption of vector data. The details of the security and algorithms are described in Appendix A.

The BFV scheme consists of algorithms **KeyGen**, **Enc**, **Dec**, **Add**, and **Mult**. The key generation algorithm **KeyGen**(λ) takes a security parameter λ and creates a public key \mathbf{pk} , secret key \mathbf{sk} , and relinearization key \mathbf{rlk} . The public and secret keys are respectively used to encrypt a plaintext and decrypt a ciphertext. The relinearization key is to be published and is required for homomorphic multiplication. The encryption algorithm **Enc**(\mathbf{pk}, \mathbf{m}) provides the ciphertext of a plaintext \mathbf{m} in a polynomial ring R_T . Conversely, the decryption algorithm **Dec**(\mathbf{sk}, \mathbf{ct}) recovers the plaintext from the ciphertext \mathbf{ct} in R_Q^2 . The ciphertexts of the BFV scheme must be correctly decrypted for all plaintexts in R_T with valid parameters, namely

$$\text{Dec}(\mathbf{sk}, \text{Enc}(\mathbf{pk}, \mathbf{m})) = \mathbf{m}, \forall \mathbf{m} \in R_T$$

for some λ and for any \mathbf{pk} and \mathbf{sk} generated by **KeyGen**(λ).

The BFV scheme enables evaluation of both addition and multiplication over the ciphertext space. The number of the evaluation depends on a security parameter λ .

The algorithm **Add**($\mathbf{ct}_1, \mathbf{ct}_2$) computes the homomorphic addition of ciphertexts \mathbf{ct}_1 and \mathbf{ct}_2 , and it satisfies

$$\text{Dec}(\mathbf{sk}, \text{Add}(\mathbf{ct}_1, \mathbf{ct}_2)) = [\mathbf{m}_1 + \mathbf{m}_2]_T$$

for $\mathbf{ct}_1 = \text{Enc}(\mathbf{pk}, \mathbf{m}_1)$ and $\mathbf{ct}_2 = \text{Enc}(\mathbf{pk}, \mathbf{m}_2)$. Similarly, the algorithm **Mult**($\mathbf{rlk}, \mathbf{ct}_1, \mathbf{ct}_2$) computes the homomorphic multiplication, and it holds

$$\text{Dec}(\mathbf{sk}, \text{Mult}(\mathbf{rlk}, \mathbf{ct}_1, \mathbf{ct}_2)) = [\mathbf{m}_1 \mathbf{m}_2]_T.$$

Note that the number of elements in a ciphertext increases in every homomorphic multiplication. Furthermore, ciphertexts with different numbers of elements cannot be added to each other. For instance, a ciphertext $\mathbf{ct}_3 = \text{Mult}(\mathbf{rlk}, \mathbf{ct}_1, \mathbf{ct}_2)$ has three elements. We cannot compute **Add**($\mathbf{ct}_1, \mathbf{ct}_3$) and **Add**($\mathbf{ct}_2, \mathbf{ct}_3$) because \mathbf{ct}_1 and \mathbf{ct}_2 have two elements. Relinearization, which requires a relinearization key \mathbf{rlk} , is the process of reducing the number of ciphertext elements to two. We assume that relinearization is performed after every homomorphic multiplication.

The security of the BFV scheme is based on the ring learning with errors problem. The problem is believed to be computationally hard to solve, even when a quantum computer is used [23]. In the following, we omit the keys of the arguments for simplicity.

3 Input-Output History Feedback Controller

This section proposes a novel controller representation to implement an encrypted dynamic controller. The proposed scheme represents any linear time-invariant controller without controller states, instead of using the history of inputs and outputs of the controller.

Given a discrete-time system

$$\begin{cases} x_{t+1} = A_p x_t + B_p u_t, \\ y_t = C_p x_t, \end{cases} \quad (1)$$

where $t \geq 0$ is a time, $x \in \mathbb{R}^n$ is a state, $u \in \mathbb{R}^m$ is an input, and $y \in \mathbb{R}^\ell$ is an output. This study considers encrypting the following linear time-invariant controller based on history data to control the plant (1):

$$\begin{cases} z_{t+1} = A z_t + B y_t + E r_t, \\ u_t = C z_t + D y_t + F r_t, \end{cases} \quad (2)$$

where $z \in \mathbb{R}^p$ is a controller state, and $r \in \mathbb{R}^q$ is a reference input. We assume that the pair (A, C) is observable without loss of generality. If the pair is not observable, the controller can be reconstructed as minimal realization. This section presents another representation of (2) without using its state z , called the *input-output history feedback controller (IOHFC) representation*, in order to

enable an encrypted controller of (2) to operate for an infinite time horizon without overflow.

Let $[d_k]_{t_1}^{t_2} := [d_{t_1}^\top \cdots d_{t_2}^\top]^\top$ be a stacked vector of time-series data d_k for $t_1 \leq k \leq t_2$. With this notation, the following equations are obtained from (2):

$$z_t = A^L z_{t-L} + R_L [y_k]_{t-1}^{t-L} + S_L [r_k]_{t-1}^{t-L}, \quad (3)$$

$$[u_k]_{t-1}^{t-L} = V_L z_{t-L} + H_L [y_k]_{t-1}^{t-L} + J_L [r_k]_{t-1}^{t-L}, \quad (4)$$

where $L > 0$ is a data length, $V_L := [C^\top \cdots (CA^{L-1})^\top]^\top \in \mathbb{R}^{Lm \times p}$, $R_L := [A^{L-1}B \cdots B] \in \mathbb{R}^{p \times L\ell}$, $S_L := [A^{L-1}E \cdots E] \in \mathbb{R}^{p \times Lq}$, and

$$H_L := \begin{bmatrix} D & O & \cdots & O & O \\ CB & D & \cdots & O & O \\ \vdots & \vdots & \ddots & \vdots & \vdots \\ CA^{L-2}B & CA^{L-1}B & \cdots & CB & D \end{bmatrix} \in \mathbb{R}^{Lm \times L\ell},$$

$$J_L := \begin{bmatrix} F & O & \cdots & O & O \\ CE & F & \cdots & O & O \\ \vdots & \vdots & \ddots & \vdots & \vdots \\ CA^{L-2}E & CA^{L-1}E & \cdots & CE & F \end{bmatrix} \in \mathbb{R}^{Lm \times Lq}.$$

Assume that L is chosen to satisfy $\text{rank } V_L = n$. Then, there exists the Moore-Penrose inverse V_L^+ of V_L such that $V_L^+ V_L = I$ because V_L is full column rank. Thus, it follows from (4) that

$$z_{t-L} = V_L^+ [u_k]_{t-1}^{t-L} - V_L^+ H_L [y_k]_{t-1}^{t-L} - V_L^+ J_L [r_k]_{t-1}^{t-L}. \quad (5)$$

By substituting (5) into (3), the controller state z at time t can be represented as

$$z_t = (S_L - A^L V_L^+ J_L) [r_k]_{t-1}^{t-L} + (R_L - A^L V_L^+ H_L) [y_k]_{t-1}^{t-L} + A^L V_L^+ [u_k]_{t-1}^{t-L}.$$

Hence, the input u can be computed as follows.

$$u_t = K v_t, \quad (6)$$

where

$$K := \begin{bmatrix} C(S_L - A^L V_L^+ J_L) & F & C(R_L - A^L V_L^+ H_L) \\ D & CA^L V_L^+ \end{bmatrix},$$

$$v_t := \left[([r_k]_t^{t-L})^\top \quad ([y_k]_t^{t-L})^\top \quad ([u_k]_{t-1}^{t-L})^\top \right]^\top.$$

The controller (6) is another representation of the controller (2) based on the history data, and their control inputs u_t are the same after L samples. Consequently, we obtain the following theorem.

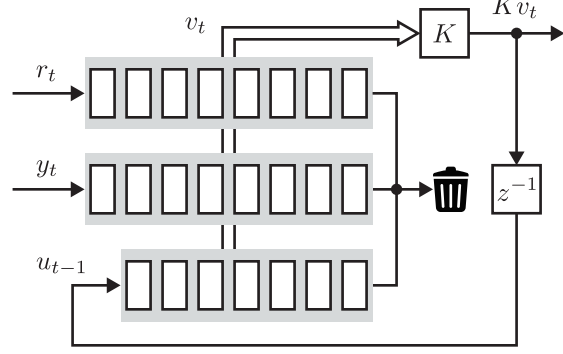


Fig. 1. Schematic picture of the IOHFC ($L = 7$).

Theorem 1 Suppose $z_t = 0$ for $t \leq 0$. For the linear time-invariant controller (2), there exists an IOHFC (6) such that its control input exactly matches that of (2) for all $t \geq 0$.

A schematic picture of the IOHFC is illustrated in Fig. 1. The controller has three queues of lengths $L+1$ and L to store history data. A reference input r and output y are transmitted to the controller from a plant at time t and added to the back end of the queues. Then, the control input u of the controller (6) is simply computed by the product between a controller gain K and a data vector v constructed from the history data. The control input is returned to the plant and appended to the back end of the queue simultaneously.

Remark 2 The proposed controller representation is a form of a vector autoregressive model with exogenous variables. Some studies have used the model to represent dynamical systems [4, 14]. However, to the best of our knowledge, few studies have applied the model to dynamic feedback controllers. Theorem 1 reveals that a dynamic controller can be represented by history data instead of the controller state without performance degradation.

4 Encrypting IOHFC

The IOHFC representation proposed in Section 3 cannot be directly employed for the implementation of encrypted dynamic controllers because the domains of the signals in a control system and a cryptosystem are different. This section presents an encoding method to deal with the difference in the domains. Additionally, we introduce a batching technique to reduce the computation costs of the encryption, which typically grow as the input and output dimensions of the system (1) increase. Using the encoding and batching technique, an efficient algorithm for matrix-vector multiplication with encrypted data is provided. Furthermore, an algorithm for the implementation of an encrypted IOHFC is proposed based on the matrix-vector multiplication algorithm to allow the controller to operate for an infinite time horizon without overflow.

4.1 Preliminaries of encoding and batching

Although the controller parameters and signals are real-number matrices and vectors, respectively, the plaintext space of the BFV scheme is a polynomial ring with coefficients of integer modulo T . Hence, the matrices and vectors should be converted into a polynomial before encryption. To this end, we first consider the following encoder and decoder to convert a real number into an integer modulo T , and vice versa:

$$\begin{aligned} \text{Ecd}_\Delta : \mathbb{R} &\rightarrow \mathbb{Z}_T : x \mapsto \lfloor [x/\Delta] \rfloor_T, \\ \text{Dcd}_\Delta : \mathbb{Z}_T &\rightarrow \mathbb{R} : z \mapsto \Delta z, \end{aligned}$$

where $\Delta > 0$ is a sensitivity for tuning the rounding errors caused by the encoding process, and the encoder and decoder operate for each element of vectors and matrices. With proper sensitivity, the elements of the matrices and vectors can be encoded and decoded with the desired precision.

Next, we consider transforming matrices and vectors of integer modulo T to the corresponding polynomials. One possible way for the transformation is to regard an element of the matrices and vectors as a polynomial of degree zero. This trivial transformation does not require additional computation processes. However, it is not efficient from the perspective of the total computation cost because an m -by- n matrix or an n -dimensional vector have the same number of polynomials to represent the plaintext, namely mn or n polynomials. The encryption and decryption algorithms should perform all polynomials, and thus a large amount of computation time and resources are required.

This study employs a batching technique for efficient transformation from matrices and vectors to polynomials. Batching based on the Chinese remainder theorem (CRT) is a technique used in the cryptography of ring learning with errors to pack multiple integers into a single polynomial plaintext. The CRT batching is effective for accelerating the computation of cryptosystems by allowing single instruction/multiple data (SIMD) operations for homomorphic evaluation [25]. The remainder of this section describes the CRT batching for the BFV scheme.

Suppose T is a prime such that $T = 1 \pmod{2N}$. From the CRT, we have the ring isomorphism [3]

$$\begin{aligned} R_T &= \mathbb{Z}_T[X]/(X - \zeta)(X - \zeta^3) \cdots (X - \zeta^{2N-1}), \\ &\cong \mathbb{Z}_T[X]/(X - \zeta) \times \cdots \times \mathbb{Z}_T[X]/(X - \zeta^{2N-1}), \\ &\cong \mathbb{Z}_T[\zeta] \times \cdots \times \mathbb{Z}_T[\zeta^{2N-1}], \\ &\cong \mathbb{Z}_T^N, \end{aligned}$$

where ζ is the primitive $2N$ th root of unity, that is, $\zeta^{2N} = 1 \pmod{T}$ and $\zeta^i \neq 1 \pmod{T}$ for $0 < i < 2N$. The

CRT batching is constructed based on this isomorphism. A canonical map from R_T to \mathbb{Z}_T^N is given as

$$\mathbf{m}(X) \mapsto [\mathbf{m}(\zeta) \ \mathbf{m}(\zeta^3) \ \cdots \ \mathbf{m}(\zeta^{2N-1})]. \quad (7)$$

The map (7) can be represented by the nega-cyclic number theoretic transform (NTT) as follows [22]:

$$\sigma^{-1} : R_T \rightarrow \mathbb{Z}_T^N : \mathbf{m} = \sum_{i=0}^{N-1} m_i X^i \mapsto [z_1 \ \cdots \ z_N], \quad (8)$$

$$\begin{bmatrix} z_1 \\ z_2 \\ \vdots \\ z_N \end{bmatrix} = \begin{bmatrix} 1 & 1 & \cdots & 1 \\ 1 & \omega & \cdots & \omega^{N-1} \\ \vdots & \vdots & \ddots & \vdots \\ 1 & \omega^{N-1} & \cdots & \omega^{(N-1)^2} \end{bmatrix} \left(\begin{bmatrix} 1 \\ \zeta \\ \vdots \\ \zeta^{N-1} \end{bmatrix} \odot \begin{bmatrix} m_0 \\ m_1 \\ \vdots \\ m_{N-1} \end{bmatrix} \right)_T,$$

where \odot denotes the Hadamard product, and ω is the primitive N th root of unity. Additionally, the inverse transformation of (8) with the inverse NTT is given as

$$\sigma : \mathbb{Z}_T^N \rightarrow R_T : [z_1 \ \cdots \ z_N] \mapsto \mathbf{m} = \sum_{i=0}^{N-1} m_i X^i, \quad (9)$$

$$\begin{bmatrix} m_0 \\ m_1 \\ \vdots \\ m_{N-1} \end{bmatrix} = \begin{bmatrix} 1 \\ \xi \\ \vdots \\ \xi^{N-1} \end{bmatrix} \odot \left(\frac{1}{N} \begin{bmatrix} 1 & 1 & \cdots & 1 \\ 1 & \pi & \cdots & \pi^{N-1} \\ \vdots & \vdots & \ddots & \vdots \\ 1 & \pi^{N-1} & \cdots & \pi^{(N-1)^2} \end{bmatrix} \begin{bmatrix} z_1 \\ z_2 \\ \vdots \\ z_N \end{bmatrix} \right)_T,$$

where $\xi = [\zeta^{-1}]_T$ and $\pi = [\omega^{-1}]_T$. Consequently, we obtain the map (9) for packing multiple integers into a single polynomial and the map (8) for unpacking the polynomial.

4.2 Matrix-vector multiplication by SIMD operations

We next present a method for secure matrix-vector multiplication by SIMD operations. With the CRT batching, element-wise addition and multiplication between two vectors $v_1, v_2 \in \mathbb{Z}_T^N$ can be evaluated by the SIMD operations over the ciphertext space as follows:

$$\begin{aligned} \sigma^{-1} \circ \text{Dec} \circ \text{Add}(\text{Enc} \circ \sigma(v_1), \text{Enc} \circ \sigma(v_2)) &= [v_1 + v_2]_T, \\ \sigma^{-1} \circ \text{Dec} \circ \text{Mult}(\text{Enc} \circ \sigma(v_1), \text{Enc} \circ \sigma(v_2)) &= [v_1 \odot v_2]_T. \end{aligned}$$

Moreover, the BFV scheme with the CRT batching allows permutations of plaintext slots, that is, the positions of the elements of an integer vector, by using the Galois automorphism sending a polynomial $\mathbf{m}(X) \in R_T$ to $\mathbf{m}(X^{2^i-1})$ [3]. We define this permutation of shifting one slot to the left as $\text{Rotate} : R_Q^2 \rightarrow R_Q^2 : \text{ct} \mapsto \text{ct}'$, and

Algorithm 1 Secure matrix-vector multiplication by SIMD operations.

Input: $M \in \mathbb{Z}_T^{m \times n}$, $v \in \mathbb{Z}_T^n$

Output: $[Mv]_T$

```

1: Let  $z_1, z_2$ , and  $z_3$  be row vectors in  $\mathbb{Z}_T^N$ 
2:  $z_1 \leftarrow [\text{vec}(M^\top)^\top \mathbf{0}_{N-mn}]$ ,  $z_2 \leftarrow [v^\top \cdots v^\top \mathbf{0}_{N-mn}]$ 
3: # Encryption
4:  $\text{ct}_1 \leftarrow \text{Enc} \circ \sigma(z_1)$ ,  $\text{ct}_2 \leftarrow \text{Enc} \circ \sigma(z_2)$ 
5: # Multiplication over the ciphertext space
6:  $\text{ct}_3 \leftarrow \text{Mult}(\text{ct}_1, \text{ct}_2)$ 
7: while  $n - 1$  times do
8:    $\text{ct}_3 \leftarrow \text{Add}(\text{ct}_3, \text{Rotate}(\text{ct}_3))$ 
9: end while
10: # Decryption
11:  $z_3 \leftarrow \sigma^{-1} \circ \text{Dec}(\text{ct}_3)$ 
12: return  $[z_{3,1} \ z_{3,n+1} \ \cdots \ z_{3,(m-1)n+1}]^\top$ 

```

it satisfies

$$\begin{aligned} & \sigma^{-1} \circ \text{Dec} \circ \text{Rotate} \circ \text{Enc} \circ \sigma([z_1 \ z_2 \ \cdots \ z_N]) \\ &= [z_2 \ \cdots \ z_N \ z_1], \end{aligned}$$

where $z_i \in \mathbb{Z}_T$ for $1 \leq i \leq N$.

Algorithm 1 is the method combined with **Add**, **Mult**, and **Rotate** to compute multiplication between a matrix and vector, and Fig. 2 is the illustration of the algorithm. The matrix M is embedded in the first mn elements of the temporary row vector z_1 such that each row of the matrix lines up (line 2). Similarly, the vector v is copied m times, and then the vectors are also embedded in z_2 . These processes are shown in Fig. 2(b). The temporary vectors are packed into single polynomials and encrypted (line 4). Using the SIMD operations, each element of the vectors is multiplied over the ciphertext space, and then the resultant vector is added with the rotation of itself $n - 1$ times (lines 6–9). The computed ciphertext is decrypted and unpacked to z_3 , and the $(i + 1)$ th elements of z_3 for $0 \leq i \leq (m - 1)n$ are extracted to construct the target vector $[Mv]_T$ (lines 11–12). The SIMD operations of the vectors and the construction of the target vector are shown in Fig. 2(c).

We employ $\text{Enc}_\Delta := \text{Enc} \circ \sigma \circ \text{Ecd}_\Delta$ and $\text{Dec}_\Delta := \text{Dcd}_\Delta \circ \sigma^{-1} \circ \text{Dec}$ for the encryption and decryption of a real-valued vector in the following.

4.3 Encrypted IOHFC with input re-encryption

Encrypting the IOHFC (6) may appear to be straightforward because leveled fully homomorphic encryption enables the evaluation of both multiplication and addition over a ciphertext space. However, the IOHFC cannot be directly implemented in an encrypted fashion, even though Algorithm 1 is used.

This is because the history data v cannot be updated when the vector is encrypted to a single ciphertext because the ciphertext cannot be altered into another one corresponding to an updated plaintext vector without decryption. Hence, this study splits the controller gain of the IOHFC (6) into block matrices for each data as follows:

$$u_t = \sum_{i=0}^L K_{r,i} r_{t-i} + \sum_{i=0}^L K_{y,i} y_{t-i} + \sum_{i=0}^{L-1} K_{u,i} u_{t-(i+1)}, \quad (10)$$

where

$$\begin{aligned} K_{r,i} &= K_{1:m, qi+1:q(i+1)}, \\ K_{y,i} &= K_{1:m, q(L+1)+\ell i+1:q(L+1)+\ell(i+1)}, \\ K_{u,i} &= K_{1:m, (q+\ell)(L+1)+mi+1:(q+\ell)(L+1)+m(i+1)}, \end{aligned}$$

and $K_{a:b,c:d}$ is a block matrix that is obtained by slicing the a th to b th rows and the c th to d th columns of K .

It should be noted that when the vectors $K_{r,i} r_{t-i}$, $K_{y,i} y_{t-i}$, and $K_{u,i} u_{t-i}$ are directly embedded into the plaintext slots, the vectors cannot be added to each other correctly over the ciphertext space because their dimensions are not necessarily the same. Fig. 3(a) is the illustration of (10) when $L = 1$, $q = 1$, $\ell = 2$, and $m = 3$. Additionally, its embedded version is shown in Fig. 3(b), and the elements corresponding to the second element of input u_t are denoted by thick boxes. As shown in the figure, if we directly embed the vectors into the plaintext slots, several components for the computation of each element of u_t are mixed after addition. Thus, the components of each element of u_t cannot be distinct, and it is impossible to construct the target vector. To avoid this issue, the data vectors are packed into single ciphertexts after zero padding, namely

$$\begin{aligned} & \text{Enc}_{\Delta_v}([r^\top \mathbf{0}_{d-q} \cdots r^\top \mathbf{0}_{d-q} \mathbf{0}_{N-md}]), \\ & \text{Enc}_{\Delta_v}([y^\top \mathbf{0}_{d-\ell} \cdots y^\top \mathbf{0}_{d-\ell} \mathbf{0}_{N-md}]), \\ & \text{Enc}_{\Delta_v}([u^\top \mathbf{0}_{d-m} \cdots u^\top \mathbf{0}_{d-m} \mathbf{0}_{N-md}]), \end{aligned}$$

where $d = \max\{q, \ell, m\}$, and Δ_v is the sensitivity of encoding the data vectors. In conjunction with this modification, the block matrices are packed after zero padding. The embedded vectors of $K_{r,i} r_{t-i}$, $K_{y,i} y_{t-i}$, and $K_{u,i} u_{t-i}$ with zero padding are shown in Fig. 3(c). Owing to this modification, the components corresponding to each element of the target vector are separated even after addition. Note that zero padding of the vectors does not increase the computation costs for the algorithm of the BFV scheme because the algorithms perform an N -dimensional vector regardless of zero padding.

We move to another problem of encrypting the controller (6) due to accumulation of sensitivities and an increase

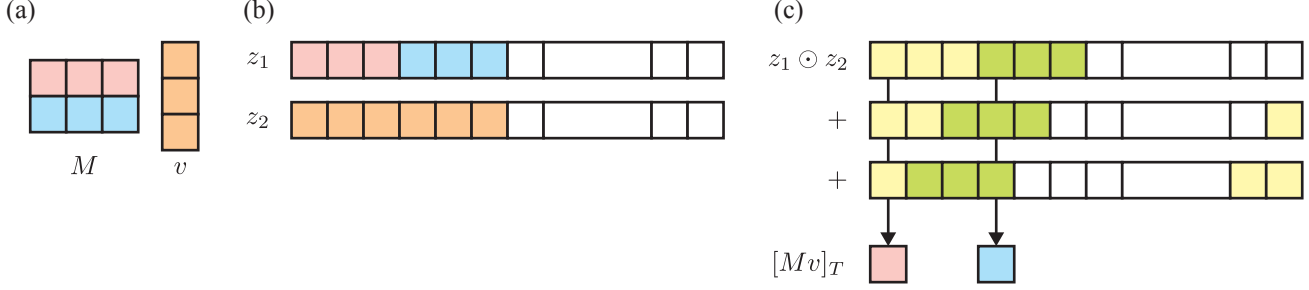


Fig. 2. Illustration of secure matrix-vector multiplication over the ciphertext space. (a) Matrix M and vector v . (b) z_1 is the vectorization of M in the plaintext slots, and z_2 is the corresponding vector of v . (c) Element-wise multiplication between z_1 and z_2 , $z_1 \odot z_2$, is added with the rotation of itself. The target vector is constructed from parts of the added vector.

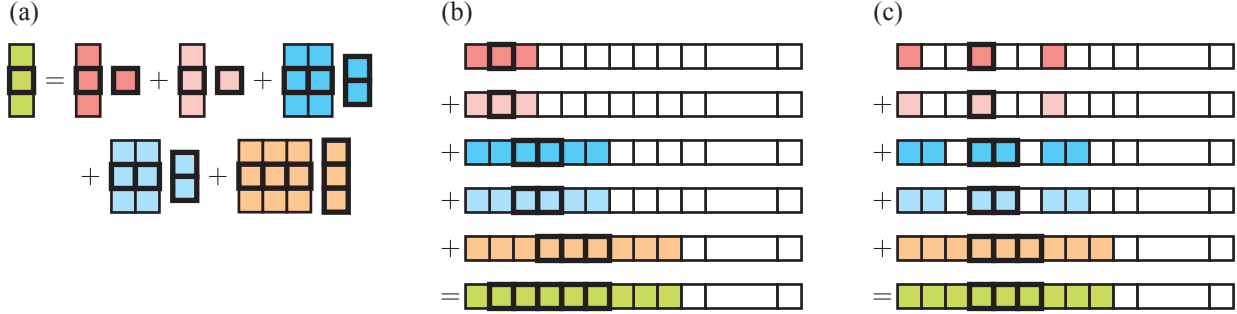


Fig. 3. Illustration of computation for the IOHFC over the ciphertext space. (a) The IOHFC (10) with $L = 1$, $q = 1$, $\ell = 2$, and $m = 3$. (b) View of the plaintext slots after element-wise multiplication when the gains and data are directly embedded into the plaintext slots. (c) View of the plaintext slots after element-wise multiplication with zero padding.

of noise in a ciphertext stored in the controller. A control input $u_t = Kv_t$ in Fig. 1 is added to the queue and recursively used to the next L times the control input computations. This operation accumulates the sensitivity Δ_K , which is used for encoding the controller gain, and increases the noise of the ciphertext in the back end of the queue. In such a case, the encrypted controller cannot operate for an infinite time horizon due to overflow, as discussed in Section 1.1. The controller (10) inherits this problem, and thus additional modifications are required.

This study considers *input re-encryption*, as shown in Fig. 4, to solve the problem of accumulation of the sensitivity. In the figure, the sensitivities in Enc, Dec and zero padding for their argument vectors are omitted for simplicity. The overall processes of the encrypted control system are described in Algorithm 2. Before operating the encrypted controller, a designer creates and distributes keys to the plant, operator, and controller (line 2). Additionally, he/she initializes the ciphertexts of the controller gain matrices ct_K^r , ct_K^y , ct_K^u and queues ct_r , ct_y , ct_u , which stores ciphertexts of history data (lines 3–15). The operator and plant respectively pack and encrypt the current reference input r_t and output y_t into single ciphertexts with zero padding and transmit them to the controller (lines 18–22). The controller evaluates (10) over the ciphertext space with encrypted controller gains and encrypted history data using the

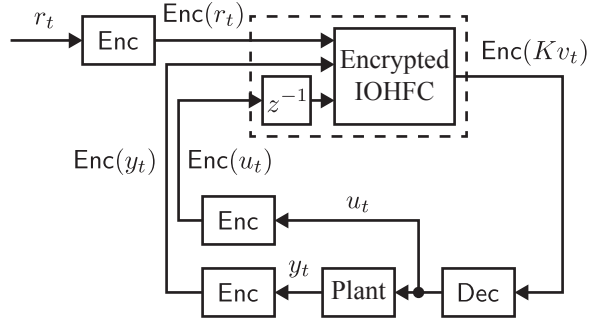


Fig. 4. Encrypted control system with IOHFC.

same methodology as Algorithm 1 (lines 24–33). The controller returns the computed ciphertext to the plant, and then the plant recovers input u_t by decrypting the ciphertext (lines 35–36). Subsequently, the input is re-encrypted and transmitted to the controller to update the history data (lines 38–45). Note that the controller (10) consists of $3L + 2$ vectors, that is, $K_{r,i}r_{t-i}$, $K_{y,i}y_{t-i}$, and $K_{u,i}u_{t-(i+1)}$. Hence, the addition of the rotation (lines 31–33), which corresponds to lines 7–9 in Algorithm 1, is conducted after aggregating with the vectors (lines 24–30).

Owing to input re-encryption, the sensitivity of each element in the queues ct_r , ct_y , and ct_u is Δ_v , even though the sensitivity of ct , i.e., the ciphertext of the target

Algorithm 2 Implementation of the encrypted IOHFC with input re-encryption.

Input: $\lambda, K, r_t, y_t, \Delta_K, \Delta_v, L, q, \ell, m, d$
Output: u_t

- 1: # Preprocessing of designer
- 2: $(\text{pk}, \text{sk}, \text{rlk}) \leftarrow \text{KeyGen}(\lambda)$, and transmit (pk, sk) , pk , and rlk to the plant, operator, and controller, respectively
- 3: **for** $i = 0, \dots, L - 1$ **do**
- 4: $\hat{K}_{r,i} \leftarrow [K_{r,i} \ O_{m \times (d-q)}]$, $\hat{K}_{y,i} \leftarrow [K_{y,i} \ O_{m \times (d-\ell)}]$
- 5: $\hat{K}_{u,i} \leftarrow [K_{u,i} \ O_{m \times (d-m)}]$
- 6: $\text{ct}_K^r[i] \leftarrow \text{Enc}_{\Delta_K}([\text{vec}(\hat{K}_{r,i}^\top)^\top \ \mathbf{0}_{N-md}])$
- 7: $\text{ct}_K^y[i] \leftarrow \text{Enc}_{\Delta_K}([\text{vec}(\hat{K}_{y,i}^\top)^\top \ \mathbf{0}_{N-md}])$
- 8: $\text{ct}_K^u[i] \leftarrow \text{Enc}_{\Delta_K}([\text{vec}(\hat{K}_{u,i}^\top)^\top \ \mathbf{0}_{N-md}])$
- 9: $\text{ct}_r[i] \leftarrow \text{Enc}_{\Delta_v}(\mathbf{0}_N)$, $\text{ct}_y[i] \leftarrow \text{Enc}_{\Delta_v}(\mathbf{0}_N)$
- 10: $\text{ct}_u[i] \leftarrow \text{Enc}_{\Delta_v}(\mathbf{0}_N)$
- 11: **end for**
- 12: $\hat{K}_{r,L} \leftarrow [K_{r,L} \ O_{m \times (d-q)}]$, $\hat{K}_{y,L} \leftarrow [K_{y,L} \ O_{m \times (d-\ell)}]$
- 13: $\text{ct}_K^r[L] \leftarrow \text{Enc}_{\Delta_K}([\text{vec}(\hat{K}_{r,L}^\top)^\top \ \mathbf{0}_{N-md}])$
- 14: $\text{ct}_K^y[L] \leftarrow \text{Enc}_{\Delta_K}([\text{vec}(\hat{K}_{y,L}^\top)^\top \ \mathbf{0}_{N-md}])$
- 15: $\text{ct}_r[L] \leftarrow \text{Enc}_{\Delta_v}(\mathbf{0}_N)$, $\text{ct}_y[L] \leftarrow \text{Enc}_{\Delta_v}(\mathbf{0}_N)$
- 16: **loop**
- 17: # Operator transmits reference input to controller
- 18: $\hat{r}_t \leftarrow [r_t^\top \ \mathbf{0}_{d-q}]$
- 19: $\text{ct}_r[L] \leftarrow \text{Enc}_{\Delta_v}([\hat{r}_t \ \dots \ \hat{r}_t \ \mathbf{0}_{N-md}])$
- 20: # Plant transmits output to controller
- 21: $\hat{y}_t \leftarrow [y_t^\top \ \mathbf{0}_{d-\ell}]$,
- 22: $\text{ct}_y[L] \leftarrow \text{Enc}_{\Delta_v}([\hat{y}_t \ \dots \ \hat{y}_t \ \mathbf{0}_{N-md}])$
- 23: # Controller returns input ciphertext ct to plant
- 24: $\text{ct} \leftarrow \text{Mult}(\text{ct}_K^r[L], \text{ct}_r[L])$
- 25: $\text{ct} \leftarrow \text{Add}(\text{ct}, \text{Mult}(\text{ct}_K^y[L], \text{ct}_y[L]))$
- 26: **for** $i = 0, \dots, L - 1$ **do**
- 27: $\text{ct} \leftarrow \text{Add}(\text{ct}, \text{Mult}(\text{ct}_K^r[i], \text{ct}_r[i]))$
- 28: $\text{ct} \leftarrow \text{Add}(\text{ct}, \text{Mult}(\text{ct}_K^y[i], \text{ct}_y[i]))$
- 29: $\text{ct} \leftarrow \text{Add}(\text{ct}, \text{Mult}(\text{ct}_K^u[i], \text{ct}_u[i]))$
- 30: **end for**
- 31: **while** $d - 1$ **times do**
- 32: $\text{ct} \leftarrow \text{Add}(\text{ct}, \text{Rotate}(\text{ct}))$
- 33: **end while**
- 34: # Plant recovers input
- 35: $w \leftarrow \text{Dec}_{\Delta_K \Delta_v}(\text{ct})$
- 36: $u_t \leftarrow [w_1 \ w_{d+1} \ \dots \ w_{(m-1)d+1}]^\top$
- 37: # Controller updates history data
- 38: **for** $i = 0, \dots, L - 1$ **do**
- 39: $\text{ct}_r[i] \leftarrow \text{ct}_r[i + 1]$, $\text{ct}_y[i] \leftarrow \text{ct}_y[i + 1]$
- 40: $\text{ct}_u[i] \leftarrow \text{ct}_u[i + 1]$
- 41: **end for**
- 42: $\text{ct}_r[L - 1] \leftarrow \text{ct}_r[L]$, $\text{ct}_y[L - 1] \leftarrow \text{ct}_y[L]$
- 43: # Plant transmits re-encrypted input to controller
- 44: $\hat{u}_t \leftarrow [u_t^\top \ \mathbf{0}_{d-m}]$
- 45: $\text{ct}_u[L] \leftarrow \text{Enc}_{\Delta_v}([\hat{u}_t \ \dots \ \hat{u}_t \ \mathbf{0}_{N-md}])$
- 46: **end loop**

vector, is $\Delta_K \Delta_v$. Moreover, ciphertexts appended to

Table 1
Number of Algorithms Executed Within a Sampling Period

	Enc	Dec	Add	Mult	Rotate
Operator	1	–	–	–	–
Plant	2	1	–	–	–
Controller	–	–	$3L + d$	$3L + 2$	$d - 1$

the back end of the queues are always fresh ciphertexts. Thus, the sensitivities and noises in each ciphertext stored in the queues do not accumulate and increase, and the encrypted control system with the IOHFC can operate for an infinite time horizon without overflow.

Remark 3 *The number of executed algorithms of the BFV scheme within a sampling period is listed in Table 1. Despite the fact that the reference input r , output y , and input u are vectors, the operator and the plant respectively execute encryption only once and twice before sending them to the controller, and the plant also performs decryption once after receiving the ciphertext from the controller. Furthermore, the number of homomorphic multiplication computed by the controller does not depend on the dimensions of the vectors. This is because the vectors are packed into single ciphertexts by the CRT batching.*

Remark 4 *An approach similar to input re-encryption has been found in the previous studies [18, 19]. However, the objective to feed back an input to a controller is different. The studies aimed to reformulate the state equation of a dynamic controller by treating it with a control input as an additional external input of the controller. In contrast, this study considers canceling the accumulation of sensitivities and the increase of noises by input re-encryption.*

5 Analysis of Quantization Effects

This section analyzes the stability and performance degradation caused by quantization in encrypted control systems when the reference input is zero. In this case, the controller gain K and the history data v are given as

$$K = [C(R_L - A^L V_L^+ H_L) \ D \ C A^L V_L^+],$$

$$v_t = [([y_k]_t^{t-L})^\top \ ([u_k]_{t-1}^{t-L})^\top]^\top.$$

Let \mathcal{Q}_Δ be the composite mapping of Enc_Δ and Dec_Δ , then

$$\begin{aligned} \mathcal{Q}_\Delta &= \text{Dec}_\Delta \circ \text{Enc}_\Delta, \\ &= \text{Dcd}_\Delta \circ \sigma^{-1} \circ \text{Dec} \circ \text{Enc} \circ \sigma \circ \text{Ecd}_\Delta, \\ &= \text{Dcd}_\Delta \circ \text{Ecd}_\Delta. \end{aligned}$$

Thus, the map \mathcal{Q}_Δ behaves as a quantizer. With the quantizer, the decrypted input of an encrypted version of the IOHFC (6) is equivalent to

$$u_t = \mathcal{Q}_{\Delta_K}(K)\mathcal{Q}_{\Delta_v}(v_t) = \bar{K}\bar{v}_t, \quad (11)$$

where $\bar{K} := \mathcal{Q}_{\Delta_K}(K)$ and $\bar{v} := \mathcal{Q}_{\Delta_v}(v)$. Quantization errors caused by the quantization are respectively bounded from above by

$$\|\bar{v}\| \leq \sqrt{(L+1)\ell + Lm\Delta_v}/2 =: \eta_v, \quad (12)$$

$$\|\bar{K}\| \leq \sqrt{(L+1)\ell m + Lm^2\Delta_K}/2 =: \eta_K, \quad (13)$$

where $\tilde{v} := \mathcal{Q}_{\Delta_v}(v) - v$ and $\tilde{K} := \mathcal{Q}_{\Delta_K}(K) - K$. The quantized controller (11) induces destabilization and performance degradation of the control system when the sensitivities are not sufficiently small. We show a condition for maintaining stability even after quantization and estimating the degree of performance degradation in the following. To this end, rewrite the system (1) as

$$\begin{cases} \mathbf{x}_{t+1} = \mathbf{A}\mathbf{x}_t + \mathbf{B}u_t, \\ v_t = \mathbf{C}_1\mathbf{x}_t, \\ y_t = \mathbf{C}_2\mathbf{x}_t, \end{cases} \quad (14)$$

where $\mathbf{x}_t = [x_{t-L}^\top \cdots x_t^\top u_{t-L}^\top \cdots u_{t-1}^\top]^\top$,

$$\mathbf{A} = \begin{bmatrix} O_{Ln \times n} & I_{Ln} & O_{Ln \times Lm} \\ O_{n \times Ln} & A_p & O_{n \times Lm} \\ O_{Lm \times (L+1)n} & O_{Lm \times m} & \begin{bmatrix} I_{(L-1)m} \\ O_{m \times (L-1)m} \end{bmatrix} \end{bmatrix},$$

$$\mathbf{B} = \begin{bmatrix} O_{Ln \times m} \\ B_p \\ O_{(L-1)m \times m} \\ I_m \end{bmatrix}, \quad \mathbf{C}_1 = \begin{bmatrix} I_{L+1} \otimes C_p & O_{(L+1)n \times Lm} \\ O_{Lm \times (L+1)n} & I_{Lm} \end{bmatrix},$$

$$\mathbf{C}_2 = \begin{bmatrix} O_{\ell \times Ln} & C_p & O_{\ell \times Lm} \end{bmatrix}.$$

The following lemma shows that the stability of the original closed-loop system is invariant even if its plant is rewritten and the IOHFC is utilized.

Lemma 5 *Suppose $z_t = 0$ for $t \leq 0$. The closed-loop system with (14) and (6) is stable if and only if that with (1) and (2) is stable.*

PROOF. We prove only the sufficient condition because the proof for the necessary condition is trivial. Given the controller (2) that stabilizes (1), then $x_t \rightarrow 0$ and $u_t \rightarrow 0$ as $t \rightarrow \infty$. Theorem 1 implies that the IOHFC (6) is equivalent to (2) for all $t \geq 0$. Thus, the

sequences $\{x_t\}_{t=0}^\infty$ and $\{u_t\}_{t=0}^\infty$ generated by (14) with (6) are the same as those in (1) with (2). This concludes state \mathbf{x} of (14) with (6) converges to zero as $t \rightarrow \infty$.

Next, the stability condition for Δ_K is derived as follows.

Theorem 6 *Given the controller (2) stabilizing the plant (1) with $z_t = 0$ for $t \leq 0$. If the sensitivity Δ_K is chosen such that*

$$\Delta_K < \beta_1 \left(-\beta_2 + \sqrt{\beta_3} \right) \quad (15)$$

with

$$\beta_1 = 2 \left(\sqrt{(L+1)\ell m + Lm^2} \|\mathbf{B}^\top \mathbf{P} \mathbf{B}\| \|\mathbf{C}_1\| \right)^{-1},$$

$$\beta_2 = \|(\mathbf{A} + \mathbf{B} \mathbf{K} \mathbf{C}_1)^\top \mathbf{P} \mathbf{B}\|,$$

$$\beta_3 = \|(\mathbf{A} + \mathbf{B} \mathbf{K} \mathbf{C}_1)^\top \mathbf{P} \mathbf{B}\|^2 + \lambda_{\min}(Q) \|\mathbf{B}^\top \mathbf{P} \mathbf{B}\|,$$

then the closed-loop system with the system (14) and the controller

$$u_t = \bar{K}v_t \quad (16)$$

is stable, where P and Q are positive definite matrices satisfying $(\mathbf{A} + \mathbf{B} \mathbf{K} \mathbf{C}_1)^\top P (\mathbf{A} + \mathbf{B} \mathbf{K} \mathbf{C}_1) - P + Q = O$.

PROOF. The closed-loop system with (14) and (16) is expressed as follows:

$$\mathbf{x}_{t+1} = \mathbf{A}\mathbf{x}_t + \mathbf{B}\bar{K}\mathbf{C}_1\mathbf{x}_t = (\mathbf{A} + \mathbf{B}\bar{K}\mathbf{C}_1)\mathbf{x}_t + \mathbf{B}\tilde{K}\mathbf{C}_1\mathbf{x}_t,$$

where $\tilde{K} = \bar{K} - K$. From Lemma 5, there always exist positive definite matrices P and Q such that $(\mathbf{A} + \mathbf{B}\bar{K}\mathbf{C}_1)^\top P (\mathbf{A} + \mathbf{B}\bar{K}\mathbf{C}_1) - P + Q = O$. Let $V(\mathbf{x}_t) = \mathbf{x}_t^\top P \mathbf{x}_t$ be a Lyapunov function candidate, then

$$\begin{aligned} & V(\mathbf{x}_{t+1}) - V(\mathbf{x}_t) \\ &= \mathbf{x}_t^\top (\mathbf{B}\tilde{K}\mathbf{C}_1)^\top \mathbf{P} \mathbf{B} \tilde{K} \mathbf{C}_1 \mathbf{x}_t + 2\mathbf{x}_t^\top (\mathbf{A} + \mathbf{B}\bar{K}\mathbf{C}_1)^\top \mathbf{P} \mathbf{B} \mathbf{K} \mathbf{C}_1 \mathbf{x}_t \\ &\quad - \mathbf{x}_t^\top Q \mathbf{x}_t, \\ &\leq \left(\|\mathbf{B}^\top \mathbf{P} \mathbf{B}\| \|\mathbf{C}_1\|^2 \|\tilde{K}\|^2 + 2\|(\mathbf{A} + \mathbf{B}\bar{K}\mathbf{C}_1)^\top \mathbf{P} \mathbf{B}\| \|\mathbf{C}_1\| \|\tilde{K}\| \right. \\ &\quad \left. - \lambda_{\min}(Q) \right) \|\mathbf{x}_t\|^2 =: g(\|\tilde{K}\|). \end{aligned}$$

The solution to the quadratic equation $g(\|\tilde{K}\|) = 0$ is

$$\|\tilde{K}\| = \frac{1}{\|\mathbf{B}^\top \mathbf{P} \mathbf{B}\| \|\mathbf{C}_1\|} \left(-\|(\mathbf{A} + \mathbf{B}\bar{K}\mathbf{C}_1)^\top \mathbf{P} \mathbf{B}\| + \sqrt{\|(\mathbf{A} + \mathbf{B}\bar{K}\mathbf{C}_1)^\top \mathbf{P} \mathbf{B}\|^2 + \lambda_{\min}(Q) \|\mathbf{B}^\top \mathbf{P} \mathbf{B}\|} \right).$$

Moreover, it follows from (13) that

$$\frac{2}{\sqrt{(L+1)\ell m + Lm}} \|\tilde{K}\| \leq \Delta_K.$$

Therefore, $g(\|\tilde{K}\|) < 0$ if Δ_K satisfies (15). This implies that $V(\mathbf{x}_{t+1}) - V(\mathbf{x}_t)$ is negative.

It should be noted that if Δ_K satisfies the condition (15), then the control system is bounded-input bounded-output stable regardless of the choice of Δ_v . This is because the closed-loop system with (14) and (11) is given as

$$\mathbf{x}_{t+1} = \mathbf{A}\mathbf{x}_t + \mathbf{B}\bar{K}\tilde{v}_t = (\mathbf{A} + \mathbf{B}\bar{K}\mathbf{C})\mathbf{x}_t + \mathbf{B}\bar{K}\tilde{v}_t,$$

and \tilde{v} is bounded by (12). Meanwhile, the output trajectory of the closed-loop system differs from the original trajectory. Moreover, a quantization error of v would further degrade the control performance. The following theorem estimates the degree of performance degradation induced by quantization of K and v .

Theorem 7 *Given the initial state x_0 and $\mathbf{x}_0 = [\mathbf{0}_{Ln} \ x_0^\top \ \mathbf{0}_{Lm}]^\top$. Suppose that $\mathbf{A} + \mathbf{B}\mathbf{K}\mathbf{C}_1$ is stable, and Δ_K satisfies the condition (15). Let y' be the output of the system (14) with the controller (11). The supremum of the error between $y(K, \mathbf{x}_0)$ and $y'(\bar{K}, \mathbf{x}_0)$ is bounded by*

$$\sup_{t>0} \|y_t(K, \mathbf{x}_0) - y'_t(\bar{K}, \mathbf{x}_0)\| \leq \beta_K c^2 \tau \gamma^{\tau-1} + \frac{\beta_v c}{1-\gamma},$$

where $\beta_K = \|\mathbf{C}_2 \mathbf{B}\| \|\mathbf{C}_1\| \|x_0\| \eta_K$, $\beta_v = \|\mathbf{C}_2\| \|\mathbf{B}\bar{K}\| \eta_v$. The parameters γ , c , and τ are determined by

$$\begin{aligned} \max\{\rho(\mathbf{A} + \mathbf{B}\mathbf{K}\mathbf{C}_1), \rho(\mathbf{A} + \mathbf{B}\bar{K}\mathbf{C}_1)\} &< \gamma < 1, \\ c &= \max_{1 \leq k \leq M} \{1, \gamma^{-k} \|(\mathbf{A} + \mathbf{B}\mathbf{K}\mathbf{C}_1)^k\|, \gamma^{-k} \|(\mathbf{A} + \mathbf{B}\bar{K}\mathbf{C}_1)^k\|\}, \\ \tau &= \lfloor -(\log \gamma)^{-1} \rfloor, \end{aligned}$$

where M is a nonnegative integer such that $\|(\mathbf{A} + \mathbf{B}\mathbf{K}\mathbf{C}_1)^k\| < \gamma^k$ and $\|(\mathbf{A} + \mathbf{B}\bar{K}\mathbf{C}_1)^k\| < \gamma^k$ for all $k \geq M$.

PROOF. Let $\mathbf{A}_{\text{cl}} = \mathbf{A} + \mathbf{B}\mathbf{K}\mathbf{C}_1$ and $\bar{\mathbf{A}}_{\text{cl}} = \mathbf{A} + \mathbf{B}\bar{K}\mathbf{C}_1$. Because \mathbf{A}_{cl} and $\bar{\mathbf{A}}_{\text{cl}}$ are assumed to be stable, there exists $M \geq 0$ such that $\|\mathbf{A}_{\text{cl}}^k\| < \gamma^k$ and $\|\bar{\mathbf{A}}_{\text{cl}}^k\| < \gamma^k$ for all $k \geq M$ [8]. Thus, $\|\mathbf{A}_{\text{cl}}^k\| \leq c\gamma^k$ and $\|\bar{\mathbf{A}}_{\text{cl}}^k\| \leq c\gamma^k$ for any k .

It follows from (14), (6), and (11) that

$$\begin{aligned} y_t(K, \mathbf{x}_0) &= \mathbf{C}_2 \mathbf{A}_{\text{cl}}^t \mathbf{x}_0, \\ y'_t(\bar{K}, \mathbf{x}_0) &= \mathbf{C}_2 \bar{\mathbf{A}}_{\text{cl}}^t \mathbf{x}_0 + \sum_{k=0}^{t-1} \mathbf{C}_2 \bar{\mathbf{A}}_{\text{cl}}^k \mathbf{B}\bar{K}\tilde{v}_{t-1-k}. \end{aligned}$$

Hence, the supremum of the error is bounded by

$$\begin{aligned} &\sup_{t>0} \|y_t(K, \mathbf{x}_0) - y'_t(\bar{K}, \mathbf{x}_0)\| \\ &\leq \sup_{t>0} \left\| \sum_{k=0}^{t-1} \mathbf{A}_{\text{cl}}^{t-1-k} \bar{\mathbf{A}}_{\text{cl}}^k \right\| \beta_K + \sup_{t>0} \left\| \sum_{k=0}^{t-1} \bar{\mathbf{A}}_{\text{cl}}^k \right\| \beta_v, \\ &\leq \sup_{t>0} \beta_K c^2 t \gamma^{t-1} + \sup_{t>0} \beta_v c \sum_{k=0}^{t-1} \gamma^k. \end{aligned}$$

For the first term of the above inequality, it follows that

$$\frac{\partial}{\partial t} t \gamma^{t-1} = \gamma^{t-1} (1 + t \log \gamma) = 0 \iff t = -(\log \gamma)^{-1},$$

where $t \neq 0$. Furthermore, the second term is calculated as

$$\sup_{t>0} \beta_v c \sum_{k=0}^{t-1} \gamma^k = \beta_v c \sum_{k=0}^{\infty} \gamma^k = \frac{\beta_v c}{1-\gamma}$$

as $\gamma < 1$. Therefore, we obtain

$$\sup_{t>0} \beta_K c^2 t \gamma^{t-1} + \sup_{t>0} \beta_v c \sum_{k=0}^{t-1} \gamma^k \leq \beta_K c^2 \tau \gamma^{\tau-1} + \frac{\beta_v c}{1-\gamma}.$$

This completes the proof.

The theorem estimates the worst-case perturbation of the output trajectory due to the encryption. It should be noted that the upper bound can be reduced by decreasing the sensitivities because β_K and β_v are linear to Δ_K and Δ_v , respectively. Moreover, the smaller γ is, the smaller the upper bound becomes. This implies that the error caused by the encryption can be decreased by making the closed-loop system more stable.

6 Numerical Simulation

This section demonstrates the feasibility of the proposed scheme using the quadruple-tank process in [15]. The model of the form (1) of the process, which is linearized around the points $h_1^0 = 12.4$ cm, $h_2^0 = 12.7$ cm, $h_3^0 = 1.8$ cm, $h_4^0 = 1.4$ cm, $v_1^0 = 3$ V, $v_2^0 = 3$ V, $\gamma_1 = 0.7$, $\gamma_2 = 0.6$ and discretized with the sampling period of 1 s,

is given as

$$A_p = \begin{bmatrix} 0.9842 & 0 & 0.0407 & 0 \\ 0 & 0.9890 & 0 & 0.0326 \\ 0 & 0 & 0.9590 & 0 \\ 0 & 0 & 0 & 0.9672 \end{bmatrix},$$

$$B_p = \begin{bmatrix} 0.0826 & 0.0010 \\ 0.0005 & 0.0625 \\ 0 & 0.0469 \\ 0.0307 & 0 \end{bmatrix}, C_p = \begin{bmatrix} 0.5 & 0 & 0 & 0 \\ 0 & 0.5 & 0 & 0 \end{bmatrix},$$

where $x_i = h_i - h_i^0$, $u_i = v_i - v_i^0$, h_i is a water level of the tank i , v_i is a voltage applied to the pump i , and the model parameters are as follows. The cross sections of the tanks are $A_1 = A_3 = 28 \text{ cm}^2$ and $A_2 = A_4 = 32 \text{ cm}^2$. The cross sections of the outlet holes are $a_1 = a_3 = 0.071 \text{ cm}^2$ and $a_2 = a_4 = 0.057 \text{ cm}^2$. The output gain is $k_c = 0.5 \text{ V/cm}$, and the input gains are $k_1 = 3.33 \text{ cm}^3/\text{Vs}$ and $k_2 = 3.35 \text{ cm}^3/\text{Vs}$. The gravitational acceleration is 981 cm/s^2 .

The parameters in (2) of the decentralized PI controller [15] used to control the process are given as

$$A = \begin{bmatrix} 1 & 0 \\ 0 & 1 \end{bmatrix}, B = \begin{bmatrix} -1 & 0 \\ 0 & -1 \end{bmatrix}, C = \begin{bmatrix} 0.1 & 0 \\ 0 & 0.0675 \end{bmatrix},$$

$$D = \begin{bmatrix} -3.0 & 0 \\ 0 & -2.7 \end{bmatrix}, E = \begin{bmatrix} 1 & 0 \\ 0 & 1 \end{bmatrix}, F = \begin{bmatrix} 3.0 & 0 \\ 0 & 2.7 \end{bmatrix},$$

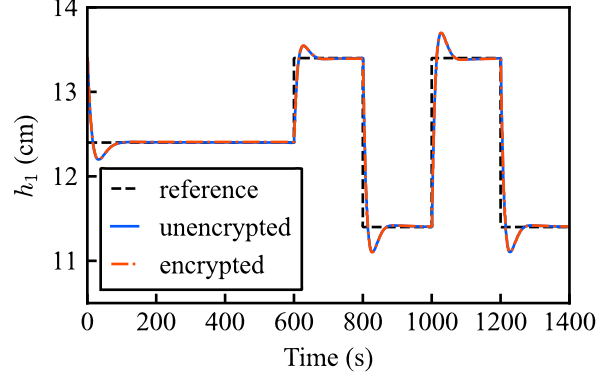
where the proportional gains are $K_1 = 3.0$ and $K_2 = 2.7$, the integral times are $T_{i1} = 30$ and $T_{i2} = 40$, and the controller is also discretized with the sampling period. The gain of the corresponding IOHFC is obtained as

$$K = \begin{bmatrix} -1.45 & 0 & -1.4 & 0 & 3.0 & 0 & 1.45 \\ 0 & -1.3163 & 0 & -1.2825 & 0 & 2.7 & 0 \\ 0 & 1.4 & 0 & -3.0 & 0 & 0.5 & 0 & 0.5 & 0 \\ 1.3163 & 0 & 1.2825 & 0 & -2.7 & 0 & 0.5 & 0 & 0.5 \end{bmatrix},$$

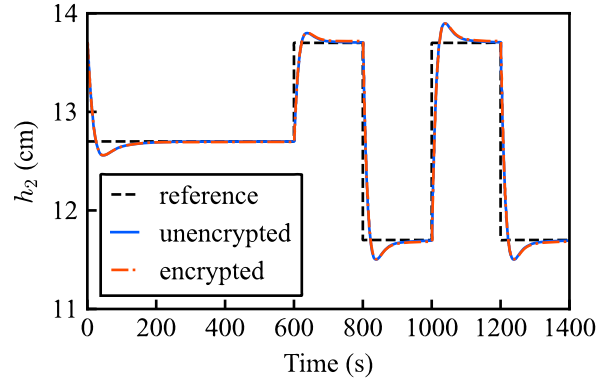
where the data length is $L = 2$.

The parameters of the BFV encryption are chosen according to the recommendation of Homomorphic Encryption Standardization¹ to satisfy $\lambda = 128$ bit security; specifically, the degree of the polynomial ring is $N = 4096$, the plaintext modulus T is a 25 bit prime, and the ciphertext modulus Q is a 109 bit integer. Additionally, the right-hand side of (15) is calculated as

¹ <https://homomorphicencryption.org/standard/>



(a) Water level in tank 1.



(b) Water level in tank 2.

Fig. 5. Comparison between the unencrypted and encrypted controls with the IOHFC.

2.3186×10^{-3} , and thus we choose $\Delta_K = \Delta_v = 10^{-3}$. From Theorem 7, the worst-case output error caused by the encryption with $x_0 = [1 \ 1 \ 1]^\top$ is bounded by 2.1145, where $\gamma = 0.9797$, $c = 11.5553$, and $\tau = 49$.

Fig. 5 depicts the results of the unencrypted and encrypted decentralized PI controls with the IOHFC representation. The initial state of the process is $x_0 = [1 \ 1 \ 1]^\top$. The reference inputs are set to $[0 \ 0]^\top$ from 0 s to 600 s and switched between $[0.5 \ 0.5]^\top$ and $[-0.5 \ -0.5]^\top$ every 200 s from 600 s to 1400 s. It should be noted that the corresponding water levels (h_1, h_2) are (12.4, 12.7), (13.4, 13.7), and (11.4, 11.7). Fig. 6 is the output error between the unencrypted and encrypted controls. These results demonstrate that the encrypted control using the IOHFC representation tracks the reference input with sufficient precision.

7 Conclusion

This paper presented a novel controller representation based on input-output history data of a dynamic controller to implement an encrypted controller with leveled fully homomorphic encryption. The proposed encrypted control scheme and algorithm enable the controller to

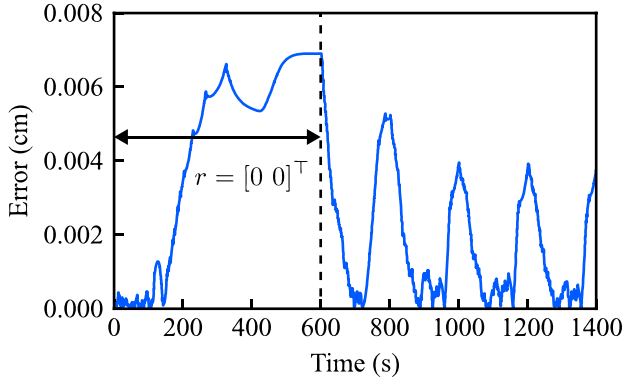


Fig. 6. Performance degradation due to encryption.

operate for an infinite time horizon without temporary decryption of the encrypted controller states. The BFV homomorphic encryption scheme with the CRT batching improves the efficiency of matrix-vector multiplication, which is included in the proposed algorithm.

We also estimated the worst-case performance degradation caused by the quantization effects due to encryption. The numerical simulation demonstrates the feasibility of the proposed encrypted control with a small performance degradation by choosing the appropriate parameters. Furthermore, the simulation results disclose that the derived theoretical estimate is slightly conservative, and so we will further analyze the effects of encryption on control performance.

Future work includes the consideration of an IOHFC representation for more complex controllers, such as nonlinear controllers. One possible way to realize a nonlinear IOHFC is use of the Koopman operator [21], which lifts a finite-dimensional nonlinear system to an infinite-dimensional linear system. The approach with appropriate truncation of a system dimension would enable application of the proposed scheme to nonlinear controllers.

Acknowledgements

This work was supported by JSPS Grant-in-Aid for JSPS Fellows Grant Number JP21J22442.

References

- [1] A. Acar, H. Aksu, A. S. Uluagac, and M. Conti. A survey on homomorphic encryption schemes: Theory and implementation. *ACM Computing Surveys*, 51(4), 2018.
- [2] A. B. Alexandru, K. Gatsis, Y. Shoukry, S. A. Seshia, P. Tabuada, and G. J. Pappas. Cloud-based quadratic optimization with partially homomorphic encryption. *IEEE Transactions on Automatic Control*, 66(5):2357–2364, 2021.
- [3] H. Chen, K. Laine, and R. Player. Simple encrypted arithmetic library – SEAL v2.1. In *Financial Cryptography and Data Security*, pages 3–18, 2017.

- [4] A. Chiuso. The role of vector autoregressive modeling in predictor-based subspace identification. *Automatica*, 43(6):1034–1048, 2007.
- [5] M. S. Darup, A. B. Alexandru, D. E. Quevedo, and G. J. Pappas. Encrypted control for networked systems: An illustrative introduction and current challenges. *IEEE Control Systems Magazine*, 41(3):58–78, 2021.
- [6] M. S. Darup, A. Redder, and D. E. Quevedo. Encrypted cooperative control based on structured feedback. *IEEE Control Systems Letters*, 3(1):37–42, 2019.
- [7] M. S. Darup, A. Redder, I. Shames, F. Farokhi, and D. E. Quevedo. Towards encrypted MPC for linear constrained systems. *IEEE Control Systems Letters*, 2(2):195–200, 2018.
- [8] D. A. Dowler. Bounding the norm of matrix powers. Master’s thesis, Brigham Young University, Provo, UT, 2013.
- [9] H. Esen, M. Adachi, D. Bernardini, A. Bemporad, D. Rost, and J. Knodel. Control as a Service (CaaS): Cloud-based software architecture for automotive control applications. In *International Workshop on the Swarm at the Edge of the Cloud*, page 13–18, 2015.
- [10] J. Fan and F. Vercauteren. Somewhat practical fully homomorphic encryption. *Cryptology ePrint Archive*, Report 2012/144, 2012.
- [11] F. Farokhi, I. Shames, and N. Batterham. Secure and private control using semi-homomorphic encryption. *Control Engineering Practice*, 67:13–20, 2017.
- [12] R. Fritz, M. Fauser, and P. Zhang. Controller encryption for discrete event systems. In *American Control Conference*, pages 5633–5638, 2019.
- [13] T. Hegazy and M. Hefeeda. Industrial automation as a cloud service. *IEEE Transactions on Parallel and Distributed Systems*, 26(10):2750–2763, 2015.
- [14] M. Jansson. Subspace identification and ARX modeling. *IFAC Proceedings Volumes*, 36(16):1585–1590, 2003.
- [15] K. H. Johansson. The quadruple-tank process: A multivariable laboratory process with an adjustable zero. *IEEE Transactions on Control Systems Technology*, 8(3):456–465, 2000.
- [16] J. Kim, C. Lee, H. Shim, J. H. Cheon, A. Kim, M. Kim, and Y. Song. Encrypting controller using fully homomorphic encryption for security of cyber-physical systems. *IFAC-PapersOnLine*, 49(22):175–180, 2016.
- [17] J. Kim and H. Shim. Encrypted state estimation in networked control systems. In *IEEE Conference on Decision and Control*, pages 7190–7195, 2019.
- [18] J. Kim, H. Shim, and K. Han. Dynamic controller that operates over homomorphically encrypted data for infinite time horizon. arXiv:1912.07362, Dec 2019.
- [19] J. Kim, H. Shim, and K. Han. Design procedure for dynamic controllers based on LWE-based homomorphic encryption to operate for infinite time horizon. In *IEEE Conference on Decision and Control*, pages 5463–5468, 2020.
- [20] K. Kogiso and T. Fujita. Cyber-security enhancement of networked control systems using homomorphic encryption. In *IEEE Conference on Decision and Control*, pages 6836–6843, 2015.
- [21] B. O. Koopman. Hamiltonian systems and transformation in Hilbert space. *Proceedings of the National Academy of Sciences*, 17(5):315–318, 1931.
- [22] P. Longa and M. Naehrig. Speeding up the number theoretic transform for faster ideal lattice-based cryptography. *Cryptology ePrint Archive*, Report 2016/504, 2016.

- [23] V. Lyubashevsky, C. Peikert, and O. Regev. On ideal lattices and learning with errors over rings. In *EUROCRYPT*, page 1–23, 2010.
- [24] C. Murguia, F. Farokhi, and I. Shames. Secure and private implementation of dynamic controllers using semi-homomorphic encryption. *IEEE Transactions on Automatic Control*, 65(9):3950–3957, 2020.
- [25] N. P. Smart and F. Vercauteren. Fully homomorphic SIMD operations. *Designs, Codes and Cryptography*, 71(1):57–81, 2014.
- [26] J. Suh and T. Tanaka. Encrypted value iteration and temporal difference learning over leveled homomorphic encryption. In *American Control Conference*, pages 2555–2561, 2021.
- [27] K. Teranishi, M. Kusaka, N. Shimada, J. Ueda, and K. Kogiso. Secure observer-based motion control based on controller encryption. In *American Control Conference*, pages 2978–2983, 2019.
- [28] K. Teranishi, N. Shimada, and K. Kogiso. Stability analysis and dynamic quantizer for controller encryption. In *IEEE Conference on Decision and Control*, pages 7184–7189, 2019.
- [29] A. Vick, V. Vonásek, R. Pěnička, and J. Krüger. Robot control as a service – towards cloud-based motion planning and control for industrial robots. In *International Workshop on Robot Motion and Control*, pages 33–39, 2015.

A BFV encryption scheme

The ring learning with errors (RLWE) problem is defined as follows [23].

Definition 8 (RLWE) *Given a security parameter λ . Let $Q = Q(\lambda) \geq 2$ be an integer, $M = M(\lambda)$ be a power of 2, and $\chi = \chi(\lambda)$ be a distribution over $R = \mathbb{Z}[X]/(\Phi_{M(\lambda)}(X))$, where $\Phi_M(X)$ is the M th cyclotomic polynomial. Sample $\mathbf{s} \leftarrow R_Q$ randomly, and define the distribution $D(\mathbf{s}, Q, \chi)$ obtained by outputting $([\mathbf{as} + \mathbf{e}]_Q, \mathbf{a})$ with random sampling $\mathbf{a} \leftarrow R_Q$ and $\mathbf{e} \leftarrow \chi$. The RLWE problem is to distinguish between $D(Q, \mathbf{s}, \chi)$ and the uniform distribution over R_Q^2 . The RLWE assumption is the assumption that the distributions are computationally indistinguishable.*

The BFV leveled fully homomorphic encryption [10] is constructed based on the RLWE assumption as follows:

- **KeyGen**(λ): Choose $N(\lambda)$, $Q(\lambda)$, $T(\lambda)$, $W(\lambda)$, and $\chi(\lambda)$. Randomly sample $\mathbf{s} \leftarrow R_2$, $\mathbf{a} \leftarrow R_Q$, $\mathbf{e} \leftarrow \chi$, $\mathbf{a}'_i \leftarrow R_Q$ and $\mathbf{e}'_i \leftarrow \chi$ for $0 \leq i \leq \ell = \lfloor \log_W(Q) \rfloor$. Set

$$\begin{aligned} \text{sk} &= \mathbf{s}, & \text{pk} &= ([-\mathbf{as} + \mathbf{e}]_Q, \mathbf{a}), \\ \text{rlk} &= [([-\mathbf{a}'_i \mathbf{s} + \mathbf{e}'_i] + W^i \mathbf{s}^2)_Q, \mathbf{a}'_i] \mid 0 \leq i \leq \ell. \end{aligned}$$

Output $(\text{sk}, \text{pk}, \text{rlk})$.

- **Enc**(pk, \mathbf{m}): A plaintext space is R_T . Let $\Delta = \lfloor Q/T \rfloor$, $\mathbf{p}_0 = \text{pk}[0]$, and $\mathbf{p}_1 = \text{pk}[1]$. Randomly sample $\mathbf{u} \leftarrow R_2$, and $\mathbf{e}_0, \mathbf{e}_1 \leftarrow \chi$. Output

$$\text{ct} = ([\mathbf{p}_0 \mathbf{u} + \mathbf{e}_0 + \Delta \mathbf{m}]_Q, [\mathbf{p}_1 \mathbf{u} + \mathbf{e}_1]_Q).$$

- **Dec**(sk, ct): A ciphertext space is R_Q^2 . Let $\mathbf{c}_0 = \text{ct}[0]$, $\mathbf{c}_1 = \text{ct}[1]$, and $\mathbf{s} = \text{sk}$. Output

$$\mathbf{m} = [\lfloor (T/Q)[\mathbf{c}_0 + \mathbf{c}_1 \mathbf{s}]_Q \rfloor]_T.$$

- **Add**(ct_1, ct_2): Let $\mathbf{c}_{10} = \text{ct}_1[0]$, $\mathbf{c}_{11} = \text{ct}_1[1]$, $\mathbf{c}_{20} = \text{ct}_2[0]$, and $\mathbf{c}_{21} = \text{ct}_2[1]$. Output

$$\text{ct}_{\text{Add}} = ([\mathbf{c}_{10} + \mathbf{c}_{20}]_Q, [\mathbf{c}_{11} + \mathbf{c}_{21}]_Q).$$

- **Mult**($\text{rlk}, \text{ct}_1, \text{ct}_2$): Let $\mathbf{c}_{10} = \text{ct}_1[0]$, $\mathbf{c}_{11} = \text{ct}_1[1]$, $\mathbf{c}_{20} = \text{ct}_2[0]$, and $\mathbf{c}_{21} = \text{ct}_2[1]$. Compute

$$\begin{aligned} \mathbf{c}_0 &= [\lfloor (T/Q)(\mathbf{c}_{10} \mathbf{c}_{20}) \rfloor]_Q, \\ \mathbf{c}_1 &= [\lfloor (T/Q)(\mathbf{c}_{10} \mathbf{c}_{21} + \mathbf{c}_{11} \mathbf{c}_{20}) \rfloor]_Q, \\ \mathbf{c}_2 &= [\lfloor (T/Q)(\mathbf{c}_{11} \mathbf{c}_{21}) \rfloor]_Q. \end{aligned}$$

Output $\text{ct}_{\text{Mult}} = \text{Relin}(\text{rlk}, \mathbf{c}_0, \mathbf{c}_1, \mathbf{c}_2)$.

- **Relin**($\text{rlk}, \mathbf{c}_0, \mathbf{c}_1, \mathbf{c}_2$): Let $\mathbf{r}_{i0} = \text{rlk}[i][0]$ and $\mathbf{r}_{i1} = \text{rlk}[i][1]$ for $0 \leq i \leq \ell$. Write $\mathbf{c}_2 = \sum_{i=0}^{\ell} \mathbf{c}_2^{(i)} W^i$ with $\mathbf{c}_2^{(i)} \in R_W$, where W is totally independent of T . Output

$$\text{ct} = \left(\left[\mathbf{c}_0 + \sum_{i=0}^{\ell} \mathbf{r}_{i0} \mathbf{c}_2^{(i)} \right]_Q, \left[\mathbf{c}_1 + \sum_{i=0}^{\ell} \mathbf{r}_{i1} \mathbf{c}_2^{(i)} \right]_Q \right).$$